Temporal Renormalization and the Critical-like Behavior in Supercooled Liquids

Dianmo Zhang[1,2], Deyan Sun[3*], and Xingao Gong[1*]

[1]*Key Laboratory for Computational Physical Sciences (MOE), Institute of Computational Physics, Fudan University, Shanghai 200433, China*
[2]*Department of Physics, College of Physics and Information Engineering, Fuzhou University, Fuzhou 350108, China*
[3]*School of Physics and Electronic Science, East China Normal University, Shanghai 200241, China*

(Received 4 November 2025; accepted manuscript online 27 January 2026)

Inspired by the Kadanoff transformation in the standard renormalization group theory, we propose a temporal renormalization scheme. A Boltzmann factor that explicitly depends on the renormalized timescale is constructed, permitting thermodynamic quantities to be evaluated self-consistently across different timescales. By applying the scheme to the long-time dynamics of supercooled liquids, we uncover critical-like behaviors in supercooled liquids with three characteristic renormalization timescales: At the first timescale s_α, the system appears to be "thermodynamically frozen", i.e., the energy fluctuation becomes temperature-independent throughout the supercooled regime. At the second timescale s_β, the third-order moment of the energy distribution reaches a maximum, and s_β is nearly temperature-independent. At the third timescale s_γ, the third-order moment of the energy distribution passes through a minimum, and s_γ diverges as a power law, $s_\gamma \sim |T - T_c|^{-\gamma}$. The scaling relations may reveal an intrinsic behavior in supercooled liquids, highlighting their unique features. The current findings also demonstrate that temporal renormalization provides a powerful lens for investigating timescale-specific dynamics.

DOI: 10.1088/0256-307X/43/2/020002 CSTR: 32039.14.0256-307X.43.2.020002

1. Introduction. In condensed matters, a wealth of fascinating phenomena is inseparable from dynamical or relaxation processes occurring at various timescales.[1–9] The timescale-specific dynamics could also be decisive in some processes or phenomena, which are particularly common and critical in non-equilibrium and complex systems.[10–17] Standard statistical mechanics, however, encodes no explicit time variable in the partition function.[18] As a result, neither the timescales themselves nor their influence on thermodynamic quantities can be read directly from the partition function. Therefore, constructing a formalism that makes this link explicit remains a central challenge.[19–21]

For most time-dependent problems, the central obstacle is the accurate treatment of long-timescale processes.[22–27] The long-time dynamical events usually exhibit relatively weak signals, so their signatures are easily overwhelmed by rapid thermal fluctuations and fast processes. Supercooled liquids furnish a paradigmatic example: their dynamical processes span many orders of magnitude in time. Long-time correlations are widely held to dictate the thermodynamic signature and, very plausibly, the glass transition itself.[28,29] Yet, in the absence of efficient theoretical methods that map timescale-specific dynamics to thermodynamics, the true nature of supercooled liquids and glasses remains an open question.

Disentangling thermodynamic behavior across timescales is a non-trivial task, whose principal obstacles are (i) the reliable isolation of various timescale processes or relaxations,[26,30] and (ii) the faithful projection of such timescale-specific dynamics onto thermodynamic properties.[31–33] At present, to our best knowledge, satisfactory solutions to either problem are unavailable. We note that in traditional renormalization methods, the Kadanoff transformation can highlight thermodynamic behavior at large spatial scales.[34,35] By extending the Kadanoff transformation to the temporal axis, we could obtain a temporal renormalization scheme capable of tracking thermodynamic behavior across different timescales. However, translating this spatial idea to the temporal axis is anything but straightforward. First, the partition function, which does not explicitly contain a time variable, offers no natural foothold for temporal renormalization. Second, the renormalization must leave the long-time dynamics intact; in other words, any temporal renormalization has to preserve, without distortion, the long-time dynamical imprint on thermodynamic quantities.

This work constructs a temporal renormalization formalism. Within this framework, we are able to quantify the long-time dynamical processes of supercooled liquids and discover three characteristic renormalization timescales, which should be intrinsic properties of long-time dynamics in supercooled liquids.

2. Theoretical Framework. Consider a system characterized by a time series $\{E(t)\}$ representing sequential instantaneous energies recorded throughout its temporal evolution at temperature T. This energy "trajectory" can

*Corresponding authors. Email: xggong@fudan.edu.cn; dysun@phy.ecnu.edu.cn
© 2026 Chinese Physical Society and IOP Publishing Ltd. All rights, including for text and data mining, AI training, and similar technologies, are reserved.

be obtained from molecular dynamics (MD) simulations, Monte Carlo simulations, or experimental observations. This set of infinitely long energy trajectories is assumed to originate from the temporal evolution of a system in thermal equilibrium. It encompasses two types of information: the microstates required for calculating the partition function and the dynamical correlations between these states. The occurrence probability $P[E(t)]$ of microstates associated with the energy $E(t)$ at time t is

$$P[E(t)] \propto \mathrm{e}^{-\beta E(t)}, \tag{1}$$

where $\beta = 1/(k_{\mathrm{B}}T)$. Considering a temporal transformation $\mathcal{F}$ to the original energy sequence $\{E(t)\}$, which yields a new set of time series,

$$E_s(t') = \mathcal{F}[E(t), E(t+1), \ldots, E(t+s)]. \tag{2}$$

Here, s represents the renormalization timescale. If transformation $\mathcal{F}$ can effectively eliminate dynamical processes with timescales shorter than s, the new time series $\{E_s(t)\}$ enables the investigation of long-time dynamical behavior. For formal simplicity in subsequent derivations, we adopt a discretized representation of $\{E(t)\}$.

Inspired by the Kadanoff transformation, we propose $\mathcal{F}$ as the following transformation:

$$E_s(i) = \frac{1}{s}\sum_{t=is+1}^{is+s} E(t). \tag{3}$$

Hereafter, this transformation is referred to as K_s. This transformation makes the time series into renormalization blocks of lengths and assigns the energy $E_s(i)$ to the i-th block. While K_s may not be the only admissible realization of $\mathcal{F}$, any transformation preserving long-time dynamics could be viable. However, our analysis demonstrates that K_s provides the most operationally tractable and theoretically minimal formulation. By means of the K_s transformation, we can isolate the dynamical processes whose characteristic timescales exceed s. Now the probability of a block microstate composed of s consecutive states associated with the short-time averaged energy E_s can be written as

$$P[E_s(i)] = \sum_{t=is+1}^{is+s} \mathrm{e}^{-\beta E(t)}. \tag{4}$$

Equations (3) and (4) do not introduce new physics; they merely redefine the microstates. In this work, our goal is to write $P[E_s(i)] \propto \mathrm{e}^{-\beta E_s(i)}$, thus the thermodynamic relations can be directly applied to the energy sequence $\{E_s(i)\}$. Fortunately, under reasonable approximations [details of the mathematical derivation can be found in the Supplementary Materials (SM)], we can obtain

$$P[E_s(i)] = \Theta(s,\beta)\mathrm{e}^{-\beta E_s(i)} \propto \mathrm{e}^{-\beta E_s(i)}, \tag{5}$$

where $\Theta(s,\beta)$ includes the contribution from short-time (less than s) dynamical processes and is approximately constant and independent of E_s. Now $P[E_s(i)]$ has the form of the standard Boltzmann factor, from which the thermodynamic quantities of interest can be directly calculated.

Each renormalization operation removes the correlation $\Theta(s,\beta)$ among the s consecutive states; consequently, the contribution from short-time dynamical processes is relegated to the discarded $\Theta(s,\beta)$. In practical applications of our method, the explicit form of $\Theta(s,\beta)$ is not required. Our purpose here is solely to demonstrate that $\Theta(s,\beta)$ is approximately independent of E_s for given s and β—a property sufficient for subsequent investigations.

To verify that the renormalization operation leaves the long-time dynamics intact, we compared the energy autocorrelation function [36] both before and after renormalization. Consider an original energy sequence $\{E(t)\}$ with duration $\mathcal{T}$, whose correlation function reads

$$\begin{aligned} G(t) &= \langle [E(0) - \langle E\rangle][E(t) - \langle E\rangle]\rangle \\ &= \langle E(0)E(t)\rangle - \langle E\rangle^2, \end{aligned} \tag{6}$$

where $\langle E\rangle = (1/\mathcal{T})\sum_1^{\mathcal{T}} E(t)$. Applying the renormalization procedure to this energy sequence yields a new time series $\{E_s(i)\}$, whose correlation function is

$$G_s(t) = \langle E_s(0)E_s(t)\rangle - \langle E_s\rangle^2. \tag{7}$$

According to Eq. (3), we know

$$\langle E_s\rangle = \frac{s}{\mathcal{T}}\sum_i^{\mathcal{T}/s}\frac{1}{s}\sum_{is+1}^{is+s} E(t) = \langle E\rangle. \tag{8}$$

Apparently, $\langle E_s\rangle$ does not change with the temporal renormalization. By combining Eqs. (3), (7), and (8), one readily obtains

$$\begin{aligned} G_s(t) &= \langle E_s(0)E_s(t)\rangle - \langle E_s\rangle^2 \\ &= \left\langle \left(\frac{1}{s}\sum_1^s E(t)\right)\left(\frac{1}{s}\sum_{is+1}^{is+s} E(t)\right)\right\rangle - \langle E_s\rangle^2 \\ &= \frac{1}{s^2}\sum_{\tau=(i-1)s}^{(i+1)s} (is - |\tau|)G(is+\tau). \end{aligned} \tag{9}$$

It can be seen that $G_s(t)$ is nothing but a smoothed version of $G(t)$ centered at $t = is$. Since the timescales of interest typically exceed the renormalization timescale s, correlations for $t > s$ remain less affected. Consequently, the time-renormalized partition function Z_s collects its dominant contributions from the long-time dynamics ($t > s$).

The time-renormalization scheme constructed here is precisely derived from the equilibrium state, aiming to screen the influence of dynamic processes at different timescales on thermodynamic behavior. Three systems studied in this work actually reside in a quasi-equilibrium state within the timescale of our simulations. But the scheme can be applied to any system that evolves over time, particularly to those complex systems in which dynamical processes span multiple timescales. For non-equilibrium states, although the weighting of microstates may not follow the standard Boltzmann form, one can still assign an effective weighting factor and apply this scheme.

3. Results and Discussion. In supercooled liquids, the unusual properties of the system are often governed

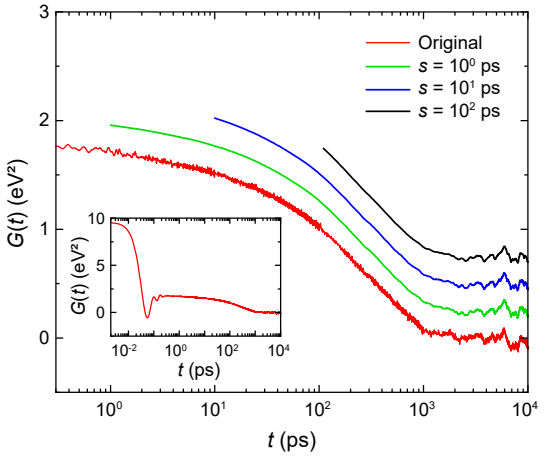

Fig. 1. Energy auto-correlation function $G_s(t)$ of the $Cu_{50}Zr_{50}$ system at $T = 800\,\mathrm{K}$. As the renormalization timescale s increases, processes below s are erased, yet all correlation behavior of the system at $t > s$ remains preserved. The $G_s(t)$ curves at $s = 10^0$, 10^1, and 10^2 ps are shifted upward by 0.25, 0.50, and $0.75\,\mathrm{eV}^2$, respectively. The inset displays the complete energy correlation function $G(t)$ without any renormalization applied.

by slow relaxation processes. These slow relaxation processes yield signals that are considerably weaker compared to those from fast relaxation processes. The temporal-renormalization method provides us with a means to study thermodynamics across different timescales in supercooled liquids. To confirm the effectiveness of the method, we performed systematic MD simulations of the $Cu_{50}Zr_{50}$ alloy, the Kob–Andersen binary Lennard–Jones (KA-BLJ) system,[37] and Al supercooled liquids using the open-source code LAMMPS[38] (details of the simulations can be found in the SM). MD simulations confirm that temporal renormalization preserves only the long-time correlations. The inset in Fig. 1 shows the energy auto-correlation function $G(t)$ in $Cu_{50}Zr_{50}$ at $T = 800\,\mathrm{K}$. In the absence of renormalization, $G(t)$ exhibits a minimum around 0.05 ps, reflecting the characteristic timescale of kinetic or thermal vibrations. Following several oscillations, $G(t)$ plateaus and then gradually decays, indicating the presence of abundant relaxation processes at this timescale. Figure 1 presents $G_s(t)$ at renormalization scales $s = 10^0$, 10^1, and 10^2 ps. Since the $G_s(t)$ curves nearly overlap with the original $G(t)$, they have been vertically offset by 0.25, 0.50, and $0.75\,\mathrm{eV}^2$, respectively. Notably, as s increases, correlations associated with time intervals shorter than s are progressively eliminated, while long-time correlations remain intact. This aligns with the above theoretical analysis and underscores the central objective of the renormalization method. Although Fig. 1 focuses on the $Cu_{50}Zr_{50}$ supercooled liquid, similar behavior is observed in the other two systems.

In the supercooled liquid regime, a special renormalization timescale—denoted as the first characteristic renormalization timescale s_α—is identified, in which the second moment of the energy distribution $D_2(s) = \langle E_s^2\rangle - \langle E_s\rangle^2$ becomes independent of temperature (more details about $D_2(s)$ can be found in the SM). Figure 2 presents contour

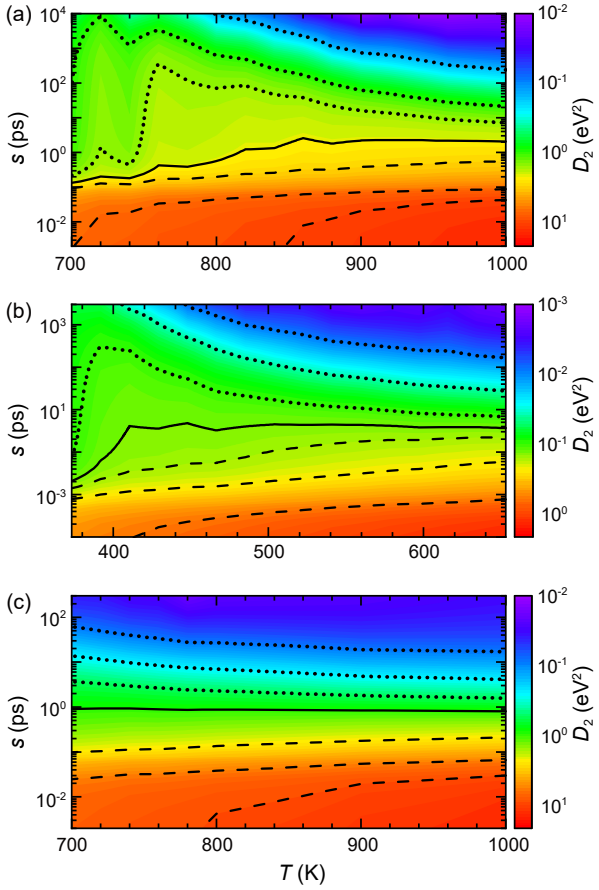

Fig. 2. Contour plots of D_2 versus s and T in (a) $Cu_{50}Zr_{50}$, (b) KA-BLJ, and (c) Al. In the supercooled regime, the contour lines tilt downward with decreasing temperature for small s (dashed line), while for large s, the contour lines rise with decreasing temperature (dotted line). Therefore, there exists a special renormalization timescale, i.e., the first characteristic renormalization timescale s_α, such that $D_2(s = s_\alpha)$ remains independent of temperature (solid line).

plots of $D_2(s)$ versus s for three distinct systems. In the supercooled regime, for small s, the contour lines tilt downward with decreasing temperature (dashed line), while for large s, they shift upward (dotted line). This behavior implies the existence of s_α, at which $D_2(s = s_\alpha)$ remains constant across temperatures (solid line). From the contour plots, this special renormalization timescale is determined to be $s_\alpha \approx 2.2$ ps, 3.8 ps, and 0.9 ps for $Cu_{50}Zr_{50}$, KA-BLJ, and Al, respectively.

Figure 3(a) illustrates the temperature dependence of $D_2(s_\alpha)$ in $Cu_{50}Zr_{50}$ at s_α. In the high-temperature region ($T > 1200\,\mathrm{K}$), where the system exhibits typical liquid behavior, $D_2(s_\alpha, T)$ decreases monotonically with decreasing temperature. Upon cooling to around 1200 K, the system enters the supercooled liquid regime, and $D_2(s_\alpha, T)$ becomes nearly independent of temperature, forming an extended plateau that persists down to approximately 850 K. Below this temperature, the system undergoes a glass transition, and $D_2(s_\alpha, T)$ resumes its decrease with further cooling. A similar phenomenon is also observed in KA-BLJ [Fig. 3(b)] and Al [Fig. 3(c)].

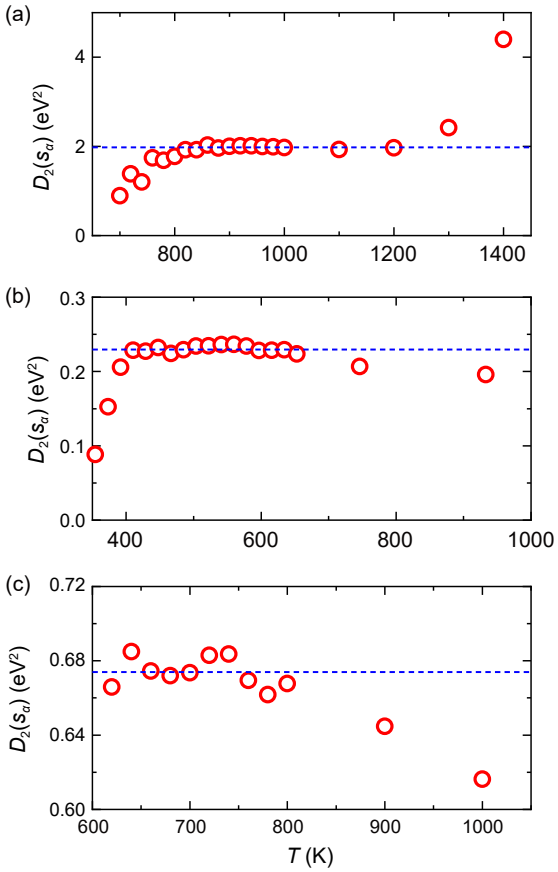

Fig. 3. The renormalized energy fluctuations D_2 obtained at the first characteristic renormalization timescale s_α. The three panels show results for (a) $Cu_{50}Zr_{50}$, (b) KA-BLJ, and (c) Al, respectively. In the supercooled liquid region, $D_2(s_\alpha)$ lies at the same height (blue dashed line) and does not vary with temperature.

The $D_2(s_\alpha, T)$ plateau emerges exclusively within the supercooled liquid regime, signaling an intrinsic signature of this metastable state. Because the evolution of D_2 with the renormalization timescale s encodes the slow dynamics in supercooled liquids, whereas the temperature-insensitive value of $D_2(s_\alpha)$ mirrors the special underlying thermodynamic behavior, it has been proven that $D_2(s)$ is a monotonically decreasing function when all microstates are uncorrelated.[39] The plateau therefore marks a dynamic–thermodynamic connection that is peculiar to the supercooled state.

At the special timescale s_α, the thermodynamic response functions become temperature-independent; i.e., the system looks "thermodynamically frozen." This result yields an intriguing picture: at s_α, the dynamical behavior in the supercooled liquid contributes identically to the energy fluctuations, implying that the long-time dynamics behavior follows identical patterns. Furthermore, the specific heat at s_α is given by

$$C(s_\alpha, T) = \frac{D_2(s_\alpha, T)}{k_B T^2} \propto T^{-2}. \tag{10}$$

We further speculate that this simple scaling relation for the renormalized specific heat may be universally present in supercooled liquids and serve as an intrinsic characteristic of such systems.

Figure 4 illustrates the third moment of the energy distribution, $D_3 = \langle (E_s - \langle E_s \rangle)^3 \rangle$ [more details about $D_3(s)$ can be found in the SM], with respect to s at different temperatures for the three systems. At small values of s, D_3 remains consistently negative, indicating a left-skewed distribution of energies. This suggests that the system predominantly occupies higher-energy states, with a pronounced tail extending into the low-energy region. As s increases, D_3 gradually rises and reaches a maximum at the second characteristic renormalization timescale, denoted as s_β, marked by open squares in Fig. 4. Notably, s_β appears to be almost independent of temperature. Since s_β closely corresponds to the timescale of thermal vibrations, we speculate that at this renormalization timescale, the contribution of vibrational entropy to the free energy may be effectively eliminated. Consequently, the energy distribution approaches a Maxwell–Boltzmann form (which becomes Gaussian in the thermodynamic limit), resulting in $D_3(s_\beta)$ being slightly positive or approximately zero.

Further increasing s reveals the third characteristic renormalization timescale, s_γ, corresponding to the minimum value of $D_3(s = s_\gamma)$ (filled circles in Fig. 4). We find that s_γ obeys the power-law scaling relation

$$s_\gamma \sim |T - T_c|^{-\gamma}. \tag{11}$$

Fitting the data points yields $T_c = 762\,\mathrm{K}$ and $\gamma = 1.93$ for the $Cu_{50}Zr_{50}$ alloy; $T_c = 385.25\,\mathrm{K}$ and $\gamma = 2.07$ for KA-BLJ; and $T_c = 590\,\mathrm{K}$ and $\gamma = 0.77$ for Al. In all three systems, T_c is consistently slightly above the glass transition temperature T_g. s_γ is therefore a previously unidentified characteristic time of supercooled liquids, distinguished from all others by both its magnitude and its critical exponent (see Fig. S1 and the corresponding discussion in the SM).

We believe that the scaling behavior associated with s_α and s_γ, identified in this work, may be unique to supercooled liquids. In contrast, standard liquids reside in thermodynamically stable states characterized by a single minimum in the free energy landscape. This corresponds to a potential energy distribution that closely approximates a single Gaussian, which becomes the standard Gaussian form in the thermodynamic limit and at infinitely high temperatures. Under such conditions, $D_2(s_\alpha)$ will decrease monotonically with decreasing temperature without exhibiting any plateaus. Similarly, s_γ cannot exist in standard liquids either. Although standard liquids can also explore multiple metabasins, the characteristic timescales from one metabasin to another are extremely short, comparable to thermal vibration timescales. As a result, in standard liquids, the energy correlation function rapidly decays to zero beyond the characteristic timescale of thermal fluctuations. At this point, the temporally renormalized energy distribution remains very close to a Gaussian distribution. However, for a Gaussian distribution, D_3 is always zero, and thus no extrema exist.

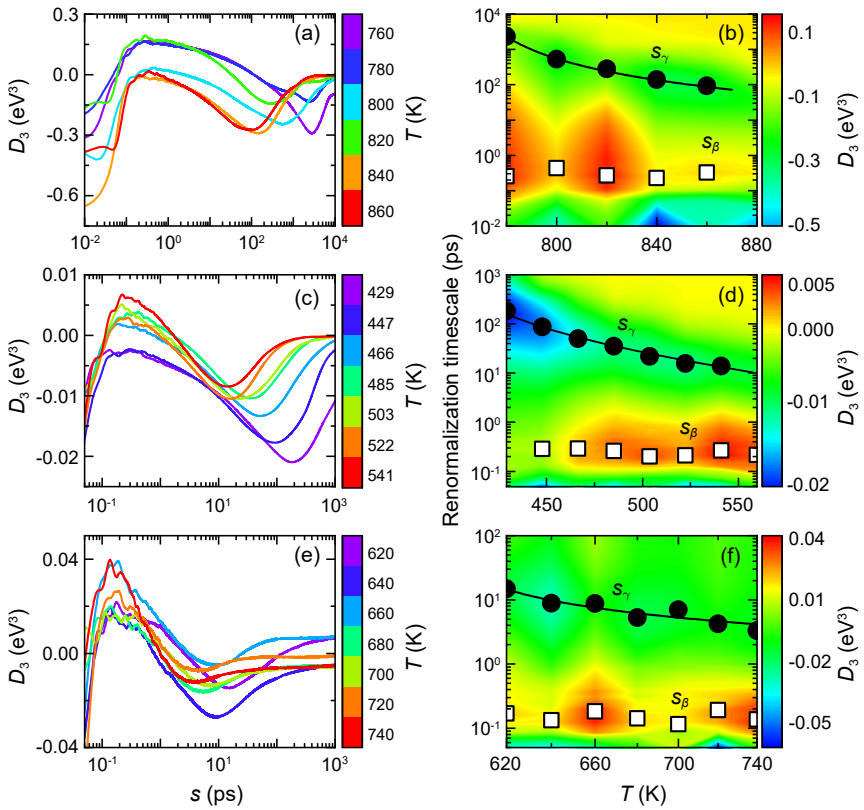

Fig. 4. Variation of D_3 with s within the supercooled liquid regime for (a) $Cu_{50}Zr_{50}$, (c) KA-BLJ, and (e) Al. As s increases, two characteristic renormalization timescales (s_β and s_γ) successively emerge, at which D_3 successively exhibits a maximum and a minimum, respectively. (b), (d), and (f) The contour plots of D_3 for $Cu_{50}Zr_{50}$, KA-BLJ, and Al, respectively. Open squares mark the second characteristic renormalization timescale s_β, which remains nearly independent of temperature; filled circles denote the third characteristic renormalization timescale s_γ, which follows a power-law scaling relation. The solid lines in the figure represent fits of s_γ using Eq. (11). The fitting critical temperatures are $T_c = 762$ K for $Cu_{50}Zr_{50}$, 385 K for KA-BLJ, and 590 K for Al, which are very close to the glass transition temperatures T_g.

4. Summary. We propose a temporal renormalization scheme. Applied to supercooled liquids, we have identified critical behavior of the supercooled liquid with three characteristic renormalization timescales. (1) A "thermodynamically frozen" plateau is observed at a specific renormalization scale s_α. At this timescale, energy fluctuations remain independent of temperature within the supercooled region. (2) At the second characteristic renormalization timescale s_β, the third moment of the energy distribution, $D_3(s_\beta)$, passes through a maximum, and s_β is almost independent of temperature. (3) The third characteristic renormalization timescale s_γ, corresponding to the minimum of $D_3(s_\gamma)$, obeys the critical scaling $s_\gamma \sim |T - T_c|^{-\gamma}$, where T_c is slightly higher than but close to the glass transition temperature. The exponent γ is distinct from all known static or dynamic exponents, signaling a previously unobserved quasi-criticality. These results reveal a unique "time-domain criticality" in supercooled liquids. Traditional glass transition criteria typically consider only one aspect—either thermodynamic or kinetic—e.g., a relaxation time reaching 10^2 s as a kinetic feature or a sudden drop in specific heat as a thermodynamic property. In this work, we clarify that the thermodynamic properties of a system are the sum of contributions from dynamics at different timescales. The glass transition may be interpreted as a phase-like transition in the temporal domain, and the characteristic renormalization timescales and the associated scaling relations serve as the new characteristic labels of supercooled liquids. This framework provides novel theoretical tools to capture timescale-specific dynamics in glass-forming liquids and, more broadly, in increasingly complex systems.

Acknowledgements. This work was supported by the National Key Research and Development Program of China (Grant No. 2022YFA1404603), and the National Natural Science Foundation of China (Grant Nos. 12274127 and 12188101).

References

[1] Scalliet C, Guiselin B, and Berthier L 2022 *Phys. Rev. X* **12** 041028
[2] Seifert U 2012 *Rep. Prog. Phys.* **75** 126001
[3] Emori S, Bauer U, Ahn S M, Martinez E, and Beach G 2013 *Nat. Mater.* **12** 611
[4] Tserkovnyak Y, Brataas A, and Bauer G 2002 *Phys. Rev. Lett.* **88** 117601
[5] Beaurepaire E, Merle J C, Daunois A, and Bigot J Y 1996 *Phys. Rev. Lett.* **76** 4250
[6] Grüner G 1988 *Rev. Mod. Phys.* **60** 1129

[7] Strungaru M, Evans R, and Chantrell R 2025 *Phys. Rev. Lett.* **135** 076701
[8] Mondal R, Rózsa L, Farle M, Oppeneer P M, Nowak U, and Cherkasskii M 2023 *J. Magn. Magn. Mater.* **579** 170830
[9] Yoo H M, Korkusinski M, Miravet D, Baldwin K W, West K, Pfeiffer L, Hawrylak P, and Ashoori R C 2023 *Nat. Commun.* **14** 7440
[10] Caprini L 2021 *J. Stat. Mech. Theory Exp.* **2021** 063202
[11] Gotze W and Sjogren L 1992 *Rep. Prog. Phys.* **55** 241
[12] Angell C A 1995 *Science* **267** 1924
[13] Debenedetti P G and Stillinger F H 2001 *Nature* **410** 259
[14] Tang Y, Liu J, Zhang J, and Zhang P 2024 *Nat. Commun.* **15** 1117
[15] Prigogine I 2017 Non-Equilibrium Statistical Mechanics (Dover Publications)
[16] Jia H H, Nakata Y, Souma S *et al.* 2025 *Phys. Rev. B* **111** 195430
[17] Dieball C and Godec A 2024 *Phys. Rev. Lett.* **133** 067101
[18] Pathria R K and Beale P D 2017 Statistical Mechanics (Elsevier)
[19] Dechant A, Garnier-Brun J, and Sasa S 2023 *Phys. Rev. Lett.* **131** 167101
[20] Delvenne J C and Falasco G 2024 *Phys. Rev. E* **109** 014109
[21] Leadbetter T, Purohit P K, and Reina C 2023 *PNAS Nexus* **2** pgad417
[22] Matsuo T and Sonoda A 2022 *Phys. Rev. E* **106** 064119
[23] Li Y, Abberton B C, Kröger M, and Liu W K 2013 *Polymers* **5** 751
[24] Tsirlin A M, Balunov A I, and Sukin I A 2025 *Entropy* **27** 649
[25] Schweizer M and Sagis L 2014 *J. Chem. Phys.* **141** 224102
[26] Schütte C, Klus S, and Hartmann C 2023 *Acta Numer.* **32** 517
[27] Lubchenko V and Wolynes P G 2004 *J. Chem. Phys.* **121** 2852
[28] Wang W H 2019 *Prog. Mater. Sci.* **106** 100561
[29] Berthier L and Biroli G 2011 *Rev. Mod. Phys.* **83** 587
[30] Gerry M, Kewming M J, and Segal D 2024 *Phys. Rev. Res.* **6** 033106
[31] Vrugt M and Wittkowski R 2019 *Phys. Rev. E* **99** 062118
[32] Hummer G and Szabo A 2001 *Proc. Natl. Acad. Sci.* **98** 3658
[33] Jarzynski C 1997 *Phys. Rev. Lett.* **78** 2690
[34] Ma S K 2018 Modern Theory of Critical Phenomena (New York: Routledge)
[35] Kadanoff L P 1966 *Phys. Phys. Fiz.* **2** 263
[36] Scargle J 1989 *Astrophys. J.* **343** 874
[37] Kob W and Andersen H C 1994 *Phys. Rev. Lett.* **73** 1376
[38] Thompson A P, Aktulga H M, Berger R *et al.* 2022 *Comput. Phys. Commun.* **271** 108171
[39] Zhang B, Zhang D M, Sun D Y, and Gong X G 2025 *Phys. Rev. E* **111** 045417